Electronic Supplementary Material (ESI) for Journal of Materials Chemistry A.

Supporting Information for

Structurally oriented black phosphorus/MXene heterostructured fibers for flexible supercapacitors with enhanced ion transport and capacitive charge storage

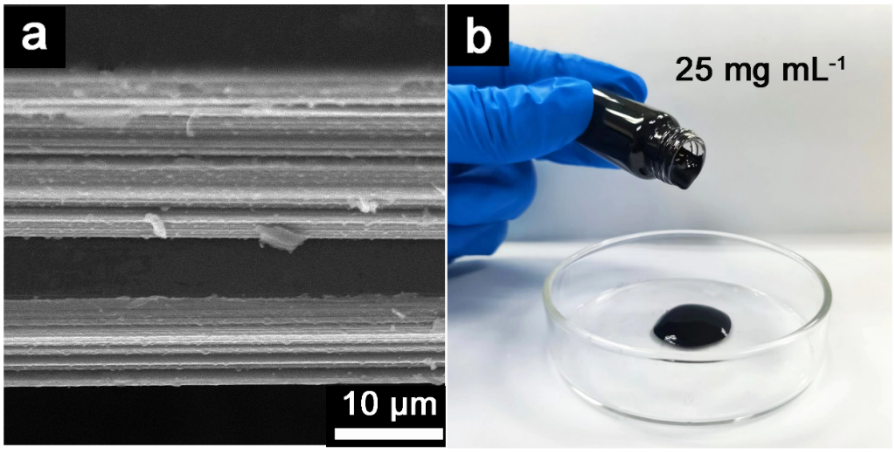

Fig. S1. (a) SEM image of unexfoliated BP bulk crystals. (b) Digital images of $Ti_3C_2T_x$ liquid crystals.

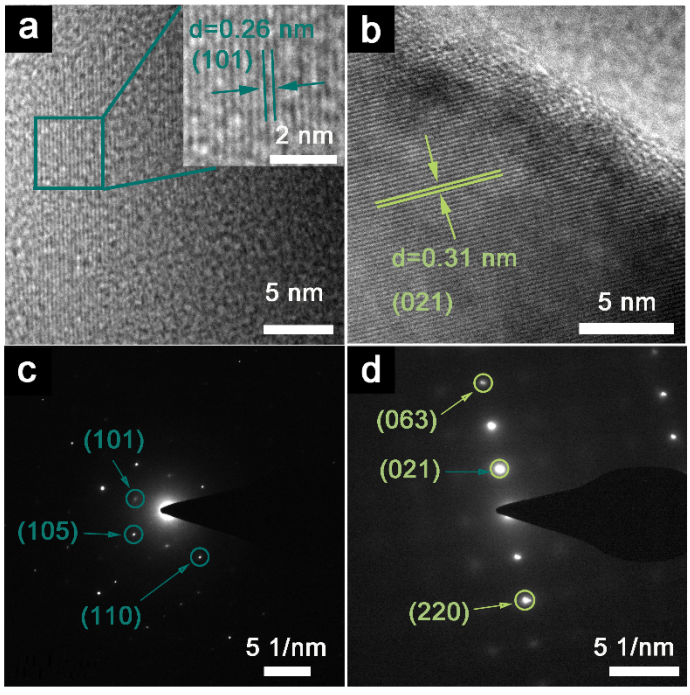

Fig. S2. HRTEM images of (a) $Ti_3C_2T_x$ nanosheets and (b) BP nanosheets. SAED patterns of (c) $Ti_3C_2T_x$ nanosheets and (d) BP nanosheets.

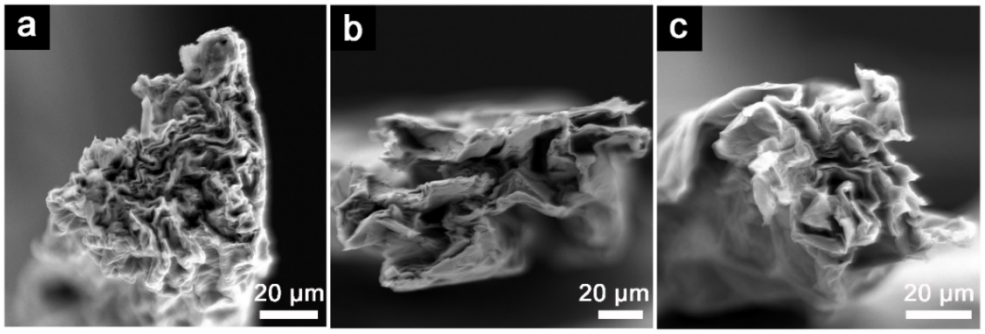

Fig. S3. Cross-section SEM images of (a) pure $Ti_3C_2T_x$ fiber, (b) 10% BP/$Ti_3C_2T_x$ and (c) 15% BP/$Ti_3C_2T_x$.

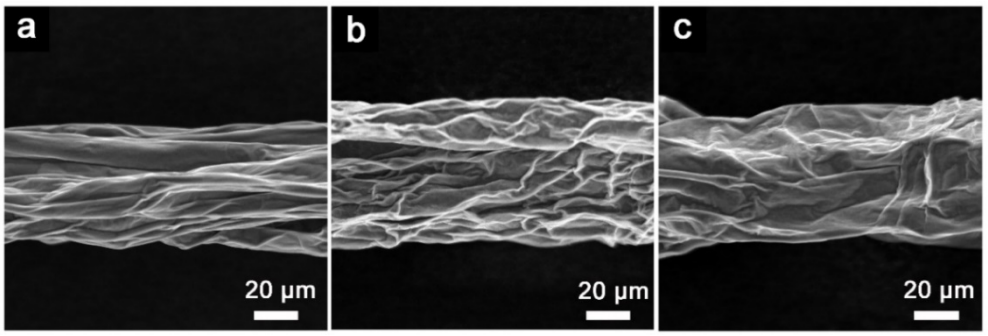

Fig. S4. Top-view SEM images of (a) pure $Ti_3C_2T_x$ fiber, (b) 10% BP/$Ti_3C_2T_x$ and (c) 15% BP/$Ti_3C_2T_x$.

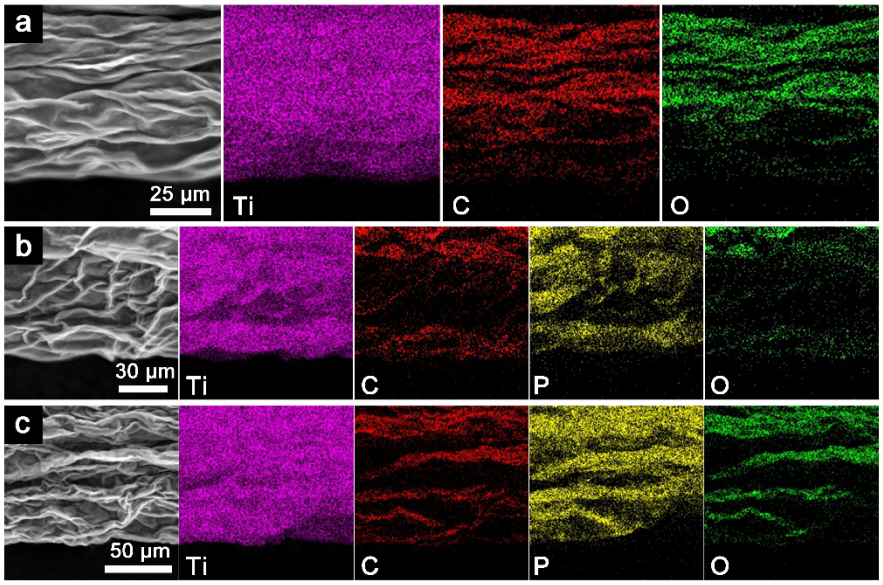

Fig. S5. Top-view EDS mapping images of (a) pure $Ti_3C_2T_x$ fiber, (b) 10% BP/$Ti_3C_2T_x$ and (c) 15% BP/$Ti_3C_2T_x$.

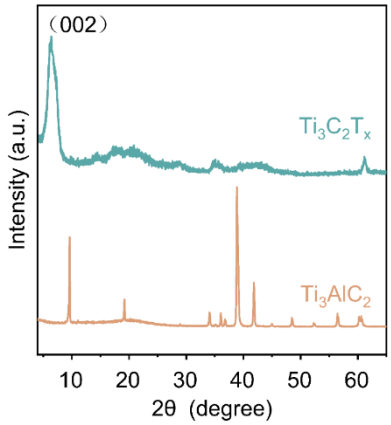

Fig. S6. XRD spectra of Ti_3AlC_2 and pure $Ti_3C_2T_x$ fiber.

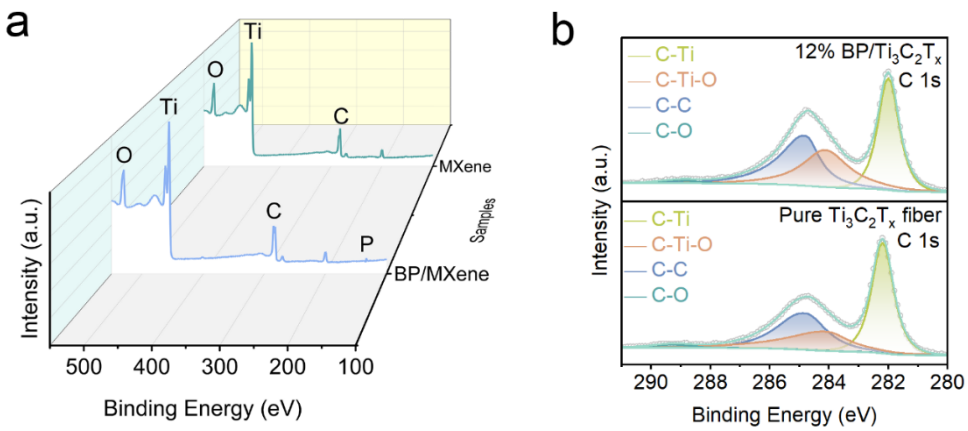

Fig. S7. (a) XPS survey spectra, and the high-resolution (b) C 1s spectra of the pure $Ti_3C_2T_x$ fiber and 12% BP/$Ti_3C_2T_x$, respectively.

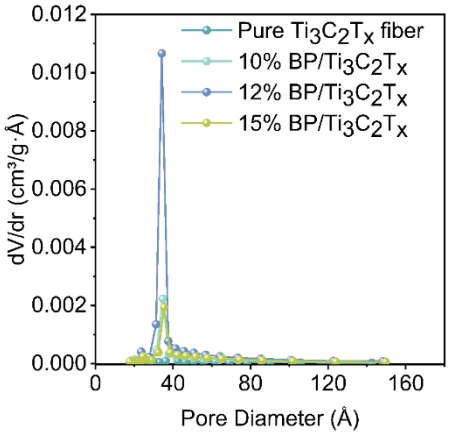

Fig. S8. Pore size distributions of the fibers.

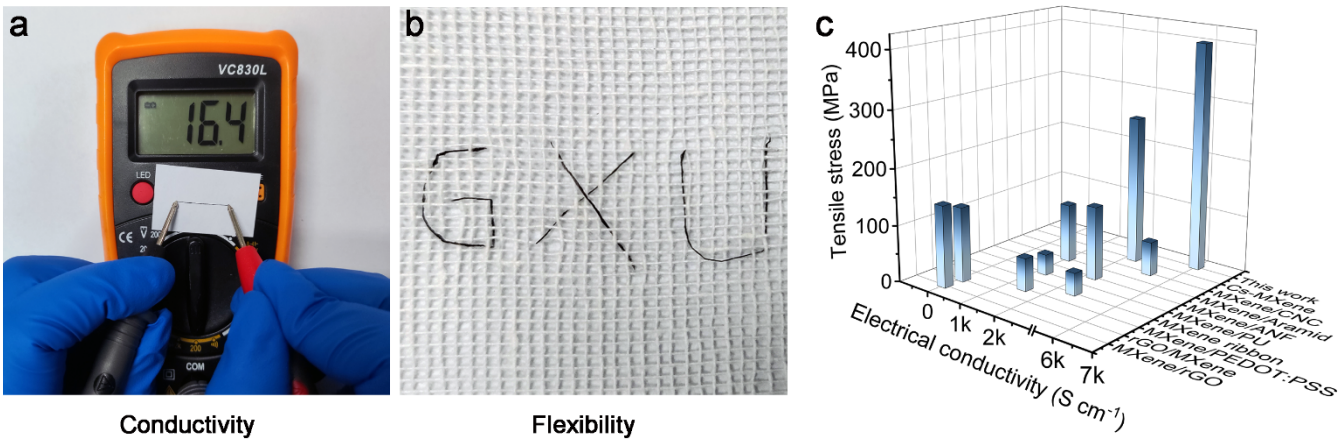

Fig. S9. (a) Fiber presenting a resistance of 16.4 Ω. (b) Fiber weaving into "GXU" shape. (c) Comparison of electrical conductivity and mechanical strength: BP/MXene heterostructured fibers were compared with previous MXene-based hybrid fibers.

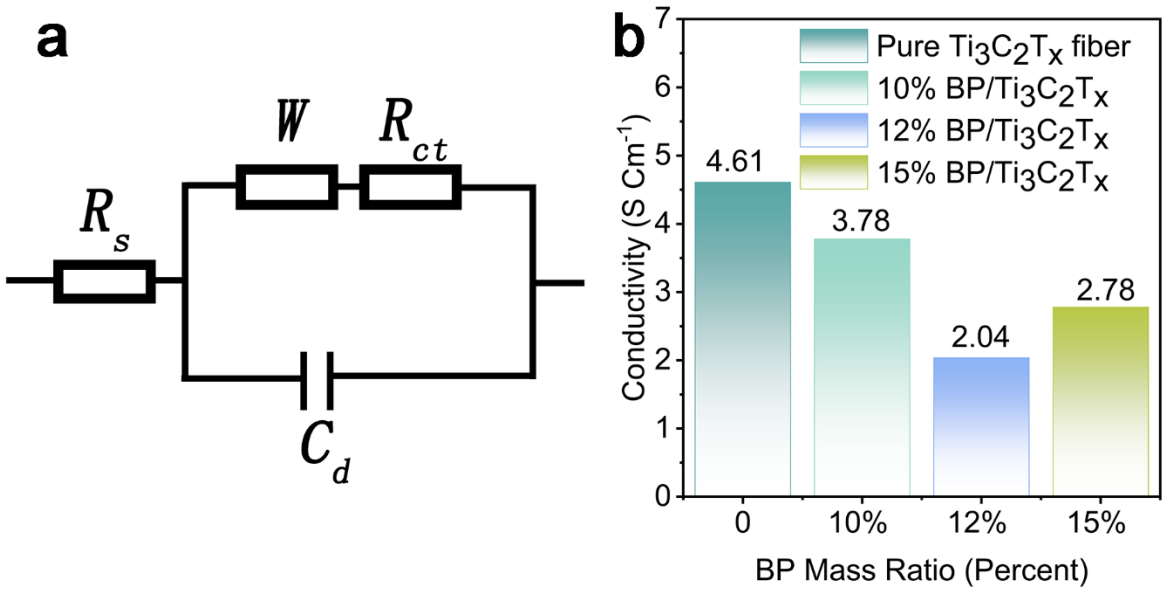

Fig. S10. (a) The equivalent circuit diagram used to fit the EIS spectrum in Fig. 4f includes R_s as series resistance, W as Warburg impedance, R_{ct} as charge transfer resistance, and C_d as intercalation capacitance. (b) ESR of the EIS spectra in Fig. 4f.

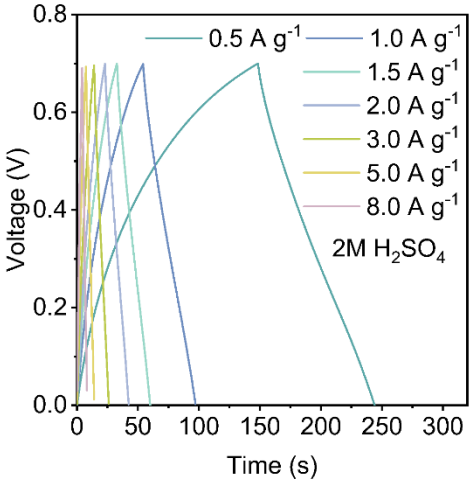

Fig. S11. GCD curves of 12% BP/$Ti_3C_2T_x$ based all-solid-state MFSCs in 2 M H_2SO_4 electrolyt at different current densities.

Table. S1. Comparison of tensile strength and electrical conductivity of MXene-based fibers with previously reported work.

Fiber	**Fabrication method**	**Tensile strength (MPa)**	**Conductivity (S cm^{-1})**	**Ref.**
MXene/rGO fiber	Wet-spinning	145	28	Ref.[1]
rGO/MXene fiber	Wet-spinning	132.5	72.3	Ref.[2]
MXene/PEDOT:PSS fiber	Wet-spinning	58.1	1489.8	Ref.[3]
MXene ribbon fiber	Wet-spinning	40	2458	Ref.[4]
MXene/PU fiber	Wet-spinning	37	1195	Ref.[5]
MXene/ANF fiber	Wet-spinning	130	2215	Ref.[6]
MXene/Aramid fiber	Wet-spinning	104	1025	Ref.[7]
MXene/CNC fiber	Wet-spinning	60	3000	Ref.[8]
Cs-MXene fiber	Wet-spinning	261.2	2215	Ref.[9]
BP/MXene fiber	Wet-spinning	401	6019	This work

Table. S2. Comparison of energy density and power density of SCs based on BP/$Ti_3C_2T_x$ heterostructured fibers with previously reported MXene based devices.

Materia	Voltage (V)	Mass loading	Energy density (mWh g^{-1})	Power density (mW g^{-1})	Ref.
BP/$Ti_3C_2T_x$ fiber	0.7	0.033 mg cm^{-1}	5.1	175	This work
			2.7	7000	
d-$Ti_3C_2T_x$ film	0.5	0.53 mg cm^{-2}	0.5	124.2	Ref.[10]
$Ti_3C_2T_x$/CNTs	0.6	0.8-1.3 mg cm^{-2}	2.8	311.0	Ref.[11]
Carbon-filled $Ti_3C_2T_x$	0.6	2.0 mg cm^{-2}	4.8	124	Ref.[12]
MXene on paper	0.6	/	0.1	46.6	Ref.[13]
PPy-MXene	0.6	/	1.3	41.1	Ref.[14]
3D-print MXene	0.6	8.5 mg cm^{-2}	2.8	75.3	Ref.[15]
Ti_2CT_x wire	0.7	0.33 mg cm^{-1}	0.3	8.8	Ref.[16]
$Ti_3C_2T_x$/V_2CT_x	0.7	/	4.9	350	Ref.[17]
			1.4	3500	Ref.[17]

References

1. Q. Yang, Z. Xu, B. Fang, T. Huang, S. Cai, H. Chen, Y. Liu, K. Gopalsamy, W. Gao and C. Gao, *J. Mater. Chem. A*, 2017, **5**, 22113-22119.
2. S. Seyedin, E. R. S. Yanza and Joselito M. Razal, *J. Mater. Chem. A*, 2017, **5**, 24076-24082.
3. J. Zhang, S. Seyedin, S. Qin, Z. Wang, S. Moradi, F. Yang, P. A. Lynch, W. Yang, J. Liu, X. Wang and J. M. Razal, *Small*, 2019, **15**, e1804732.
4. C. Zhu and F. Geng, *Carbon Energy*, 2020, **3**, 142-152.
5. S. Seyedin, S. Uzun, A. Levitt, B. Anasori, G. Dion, Y. Gogotsi and J. M. Razal, *Adv. Funct. Mater.*, 2020, **30**, 1910504
6. L. Wang, M. Zhang, B. Yang and J. Tan, *ACS Appl. Mater. Interfaces*, 2021, **13**, 41933-41945.
7. Q. Liu, A. Zhao, X. He, Q. Li, J. Sun, Z. Lei and Z. H. Liu, *Adv. Funct. Mater.*, 2021, **31**, 2010944

8. K. A. S. Usman, J. Zhang, S. Qin, Y. Yao, P. A. Lynch, P. Mota-Santiago, M. Naebe, L. C. Henderson, D. Hegh and J. M. Razal, *J. Mater. Chem. A*, 2022, **10**, 4770-4781.
9. Y. Zheng, Y. Wang, J. Zhao and Y. Li, *ACS Nano*, 2023, **17**, 2487-2496.
10. S. Xu, G. Wei, J. Li, Y. Ji, N. Klyui, V. Izotov and W. Han, *Chem. Eng. J.*, 2017, **317**, 1026-1036.
11. L. Yang, W. Zheng, P. Zhang, J. Chen, W. B. Tian, Y. M. Zhang and Z. M. Sun, *J. Electroanal. Chem.*, 2018, **830-831**, 1-6.
12. X. Zhu, X. Huang, R. Zhao, K. Liao and V. Chan, *Sustain. Energ. Fuels*, 2020, **4**, 3566-3573.
13. N. Kurra, B. Ahmed, Y. Gogotsi and H. N. Alshareef, *Adv. Energy Mater.*, 2016, **6**, 1601372.
14. J. Yan, Y. Ma, C. Zhang, X. Li, W. Liu, X. Yao, S. Yao and S. Luo, *RSC Adv.*, 2018, **8**, 39742-39748.
15. W. Yang, J. Yang, J. J. Byun, F. P. Moissinac, J. Xu, S. J. Haigh, M. Domingos, M. A. Bissett, R. A. W. Dryfe and S. Barg, *Adv. Mater.*, 2019, **31**, 1902725.
16. K. Krishnamoorthy, P. Pazhamalai, S. Sahoo and S.-J. Kim, *J. Mater. Chem. A*, 2017, **5**, 5726-5736.
17. S. Xu, H. Yang, Y. Li, H. Huang, X. Liang, Y. Wang, Q. Hu, G. Wei and Y. Yang, *Chem. Eng. J.*, 2023, **464**, 142645.